XPS (Fig. 3). The additional proton then reacts with the adsorbed OH to form H_2O ("E" in Fig. 5). In the 2 + 2–electron pathway, H_2O_2 is formed by reaction of the adsorbed OOH species with another proton ("F" in Fig. 5), followed by readsorption of H_2O_2 and its reduction by two protons to generate H_2O. The OH species detected in the post-ORR XPS measurement may arise from the four-electron mechanism, but it is also possible that the OH species next to the pyridinic N may arise from the reaction with H_2O_2 in the 2 + 2–electron mechanism. In either pathway, the carbon atoms next to pyridinic N with Lewis basicity play an important role as the active sites at which oxygen molecules are adsorbed as the initial step of the ORR.

In summary, we have demonstrated that pyridinic N in nitrogen-doped graphitic carbons creates the active sites for ORR under acidic conditions, based on studies of HOPG model catalysts and N-GNS powder catalysts. Carbon atoms next to pyridinic N are suggested to be the active sites with Lewis basicity at which O_2 molecules are adsorbed as the initial step of the ORR.

REFERENCES AND NOTES

1. K. Gong, F. Du, Z. Xia, M. Durstock, L. Dai, *Science* **323**, 760–764 (2009).
2. L. Dai, Y. Xue, L. Qu, H.-J. Choi, J.-B. Baek, *Chem. Rev.* **115**, 4823–4892 (2015).
3. J. Shui, M. Wang, F. Du, L. Dai, *Sci. Adv.* **1**, e1400129 (2015).
4. H.-W. Liang, X. Zhuang, S. Brüller, X. Feng, K. Müllen, *Nat. Commun.* **5**, 4973 (2014).
5. L. Qu, Y. Liu, J.-B. Baek, L. Dai, *ACS Nano* **4**, 1321–1326 (2010).
6. C. V. Rao, C. R. Cabrera, Y. Ishikawa, *J. Phys. Chem. Lett.* **1**, 2622–2627 (2010).
7. T. Xing *et al*., *ACS Nano* **8**, 6856–6862 (2014).
8. R. Liu, D. Wu, X. Feng, K. Müllen, *Angew. Chem.* **49**, 2565–2569 (2010).
9. H. Niwa *et al*., *J. Power Sources* **187**, 93–97 (2009).
10. H. Kim, K. Lee, S. I. Woo, Y. Jung, *Phys. Chem. Chem. Phys.* **13**, 17505–17510 (2011).
11. N. P. Subramanian *et al*., *J. Power Sources* **188**, 38–44 (2009).
12. L. Lai *et al*., *Energy Environ. Sci.* **5**, 7936–7942 (2012).
13. W. Ding *et al*., *Angew. Chem. Int. Ed.* **52**, 11755–11759 (2013).
14. Q. Li, S. Zhang, L. Dai, L. S. Li, *J. Am. Chem. Soc.* **134**, 18932–18935 (2012).
15. S. Maldonado, S. Morin, K. J. Stevenson, *Carbon* **44**, 1429–1437 (2006).
16. E. Raymundo-Piñero *et al*., *Carbon* **40**, 597–608 (2002).
17. J. R. Pels, F. Kapteijn, J. A. Moulijn, Q. Zhu, K. M. Thomas, *Carbon* **33**, 1641–1653 (1995).
18. I. Kusunoki *et al*., *Surf. Sci.* **492**, 315–328 (2001).
19. B. Li, X. Sun, D. Su, *Phys. Chem. Chem. Phys.* **17**, 6691–6694 (2015).
20. T. Kondo *et al*., *Phys. Rev. B* **86**, 035436 (2012).
21. H. Metiu, S. Chrétien, Z. Hu, B. Li, X. Sun, *J. Phys. Chem. C* **116**, 10439–10450 (2012).

ACKNOWLEDGMENTS

This work was financially supported by the New Energy and Industrial Technology Development Organization and partially supported by the Japan Science and Technology Agency–Precursory Research for Embryonic Science and Technology (JST-PRESTO) program, "New Materials Science and Element Strategy." We thank T. Kashiwagi and K. Kadowaki for support with sample etching and AFM measurements. The advice of T. Okajima and T. Ohsaka concerning the electrode preparation methods for the HOPG model catalysts is gratefully acknowledged. We thank X. Hao for assistance with sample preparation by photolithography. We thank all staff of BL07LSU of Spring-8 for assistance with surface analysis of the HOPG model catalysts. J.N. supervised the project. D.G. and C.A. prepared the model catalysts and performed XPS, AFM, and ORR measurements. R.S. performed CO_2-TPD analysis and S.S. prepared the N-GNS powder catalysts and performed ORR measurements. All authors discussed the results and D.G., T.K., and J.N. wrote the paper. The authors declare no competing financial interests.

SUPPLEMENTARY MATERIALS

www.sciencemag.org/content/351/6271/361/suppl/DC1
Materials and Methods
Supplementary Text
Figs. S1 to S10
Table S1

23 July 2015; accepted 8 December 2015
10.1126/science.aad0832

MOLECULAR FRAMEWORKS

Weaving of organic threads into a crystalline covalent organic framework

Yuzhong Liu,[1]* Yanhang Ma,[2]* Yingbo Zhao,[1]* Xixi Sun,[1] Felipe Gándara,[3] Hiroyasu Furukawa,[1] Zheng Liu,[4] Hanyu Zhu,[5] Chenhui Zhu,[6] Kazutomo Suenaga,[4] Peter Oleynikov,[2] Ahmad S. Alshammari,[7] Xiang Zhang,[5,8] Osamu Terasaki,[2,9]† Omar M. Yaghi[1,7]†

A three-dimensional covalent organic framework (COF-505) constructed from helical organic threads, designed to be mutually weaving at regular intervals, has been synthesized by imine condensation reactions of aldehyde functionalized copper(I)-bisphenanthroline tetrafluoroborate, $Cu(PDB)_2(BF_4)$, and benzidine (BZ). The copper centers are topologically independent of the weaving within the COF structure and serve as templates for bringing the threads into a woven pattern rather than the more commonly observed parallel arrangement. The copper(I) ions can be reversibly removed and added without loss of the COF structure, for which a tenfold increase in elasticity accompanies its demetalation. The threads in COF-505 have many degrees of freedom for enormous deviations to take place between them, throughout the material, without undoing the weaving of the overall structure.

Weaving, the mutual interlacing of long threads, is one of the oldest and most enduring methods of making fabric, but this important design concept has yet to be emulated in extended chemical structures. Learning how to link molecular building units by strong bonds through reticular synthesis (*1*) into weaving forms would be a boon to making materials with exceptional mechanical properties and dynamics. To successfully design weaving of chains into two- and three-dimensional (2D and 3D) chemical structures (Fig. 1, A and B), long threads of covalently linked molecules (i.e., 1D units) must be able to cross at regular intervals. It would also be desirable if such crossings serve as points of registry, so that the threads can have many degrees of freedom to move away from and back to such points without collapsing the overall structure. Structures have been made by weaving metal-organic chains (*2*), but designing well-defined materials and assembling their structures by weaving is challenging, and weaving in crystalline inorganic or covalent organic extended structures is undeveloped.

We report on a general strategy and its implementation for the designed synthesis of a woven material [covalent organic framework-505 (COF-505)]. This COF has helical organic threads interlacing to make a weaving crystal structure with the basic topology of Fig. 1B, and we show that this material has an unusual behavior in elasticity. Although terms such as interweaving (*3*), polycatenated (*2*), and interpenetrating (*4*–*6*) have been used to describe interlocking of 2D and 3D extended objects (Fig. 1, C and D), most commonly found in MOFs, we reserve the term "weaving" to describe exclusively the interlacing of 1D units to make 2D and 3D structures (Fig. 1, A and B). Weaving differs from the commonly observed interpenetrating and polycatenated frameworks because the latter are topologically interlocking

[1]Department of Chemistry, University of California, Berkeley, Materials Sciences Division, Lawrence Berkeley National Laboratory, and Kavli Energy NanoSciences Institute, Berkeley, CA 94720, USA. [2]Department of Materials and Environmental Chemistry, Stockholm University, SE-10691 Stockholm, Sweden. [3]Department of New Architectures in Materials Chemistry, Materials Science Institute of Madrid, Consejo Superior de Investigaciones Científicas, Madrid 28049, Spain. [4]Nanomaterials Research Institute, National Institute of Advanced Industrial Science and Technology (AIST), Tsukuba 305-8565, Japan. [5]NSF Nanoscale Science and Engineering Center (NSEC), University of California at Berkeley, 3112 Etcheverry Hall, Berkeley, CA 94720, USA. [6]Advanced Light Source, Lawrence Berkeley National Laboratory, Berkeley, CA 94720, USA. [7]King Abdulaziz City of Science and Technology, Post Office Box 6086, Riyadh 11442, Saudi Arabia. [8]Material Sciences Division, Lawrence Berkeley National Laboratory, 1 Cyclotron Road, Berkeley, CA 94720, USA. [9]School of Physical Science and Technology, ShanghaiTech University, Shanghai 201210, China.
*These authors contributed equally to this work. **†Corresponding author. E-mail: terasaki@mmk.su.se (O.T.); yaghi@berkeley.edu (O.M.Y.)**

(i.e., interlocking rings) (Fig. 1, C and D, insets), whereas the weaving constructs that we envision have many more degrees of freedom for enormous spatial deviations, by each of the threads, to take place independently and still preserve the underlying topology. Such freedom may enable reversible control over the mechanical properties of materials.

Our synthetic strategy is shown in Fig. 2, where we start with the aldehyde functionalized derivative of the well-known complex salt Cu(I)-bis[4,4'-(1,10-phenanthroline-2,9-diyl)dibenzaldehyde] tetrafluoroborate, $Cu(PDB)_2(BF_4)$ (Fig. 2A). The position of the aldehyde groups approximates a tetrahedral geometry and can be used in reticular synthesis as a building block to be linked with benzidine (BZ) and make an imine-bonded PDB-BZ threads weaving arrangement, with the tetrafluoroborate anions occupying the pores (Fig. 2B). The orientation of the PDB units in a mutually interlacing fashion ensures that the threads produced from linking the building units are entirely independent, with the Cu(I) ions serving as templates (points of registry) to bring those threads together in a precise manner at well-defined intervals. Because the PDB-BZ threads are topologically independent of the Cu(I) ions, the resulting woven structure is formally a COF (termed COF-505). The overall tetrahedral geometry of the aldehyde units ensures the assembly of the threads into a 3D framework (Fig. 2B). The topology of this framework is that of diamond, as expected from the principles of reticular chemistry (*1*). We show that when we remove the Cu(I) ions, the structure and its topology remain intact regardless of how the threads deviate from their points of registry, and upon remetalating, the overall structure is reversibly restored. We find a tenfold increase in elasticity when going from the metalated to the demetalated forms of the material.

The copper(I)-bisphenanthroline core of the $Cu(PDB)_2$ (without the aldehyde functionality) has been studied extensively as a discrete molecule for the formation of supramolecular complexes (*7*–*9*); however, as yet it has not been used to make extended structures, especially of the type discussed here. The tolerance for robust reaction conditions (*7*, *10*) makes this complex suitable for imine COF synthesis, especially in weak acidic conditions. Thus, the tetrahedral building unit, $Cu(PDB)_2$, was designed bearing aldehyde groups in the para positions of the two phenyl substituents (Fig. 2A). The synthesis of $Cu(PDB)_2(BF_4)$ molecular complex was carried out by air-free Cu(I) complexation of 4,4'-(1,10-phenanthroline-2,9-diyl)dibenzaldehyde, according to a previously reported procedure (*11*). The single-crystal structure of this complex revealed a distorted tetrahedral geometry around the Cu(I) center, with a dihedral angle of 57° between the two phenanthroline planes. This distortion likely arises from the π-π interaction between the phenanthroline and neighboring phenyl planes (*12*, *13*).

We synthesized COF-505 via imine condensation reactions by combining a mixture of $Cu(PDB)_2(BF_4)$ (15 mg, 0.016 mmol) and BZ (6.0 mg, 0.032 mmol) in tetrahydrofuran (THF, 1 mL) and aqueous acetic acid (6 mol/L, 100 μL). The reaction mixture was sealed in a Pyrex tube and heated at 120°C for 3 days. The resulting precipitate was collected by centrifugation, washed with anhydrous THF, and then evacuated at 120°C for 12 hours to yield 18.7 mg [94.4%, based on $Cu(PDB)_2(BF_4)$] of a dark brown crystalline solid (COF-505), which was insoluble in common polar and nonpolar organic solvents.

Fourier-transform infrared spectroscopy (FT-IR) and solid-state nuclear magnetic resonance (NMR) spectroscopy studies were performed on COF-505 to confirm the formation of imine linkages. A molecular analog of COF-505 fragment, Cu(I)-bis[(1,10-phenanthroline-2,9-diyl)bis(phenylene)bis(biphenyl)methanimine)] tetrafluoroborate, $Cu(PBM)_2(BF_4)$, was used as a model compound and synthesized by condensation of $Cu(PDB)_2(BF_4)$ and 4-aminobiphenyl (*12*). The FT-IR spectrum of COF-505 shows peaks at 1621 and 1196 cm^{-1} [1622 and 1197 cm^{-1} for $Cu(PBM)_2(BF_4)$], which are characteristic C=N stretching modes for imine bonds (*14*, *15*). Furthermore, the ^{13}C cross-polarization with magic-angle spinning (CPMAS) solid-state NMR spectrum acquired for COF-505 displays a series of peaks from 140 to 160 part per million, similar in shape and occurring at chemical shifts characteristic of those expected for C=N double bonds. To differentiate imine bonds from C=N double bonds of the phenanthroline unit, a cross-polarization and polarization inversion (CPPI) technique was applied, which leaves the signal for quaternary ^{13}C groups unchanged, whereas the residual tertiary ^{13}CH signal should approach zero (*16*). The decreased intensity of the ^{13}CH signal under these conditions confirmed the existence of imine CH=N double bond. Overall, these observations served as initial confirmation of having covalently linked imine extended threads in COF-505.

Before determining the single-crystal structure of COF-505, we studied the morphology and purity of the as-synthesized material. We found, using scanning electron microscopy (SEM), crystallites of ~200 nm are aggregated into spheres of 2 μm in diameter (Fig. 3A), which possibly arises from weak interactions of the synthesized material with the solvent, THF. No other phase was observed from SEM images taken throughout the material (*12*).

A single submicrometer-sized crystal (Fig. 3B) from this sample was studied by 3D electron diffraction tomography (3D-EDT) (*17*–*19*). One EDT data set was collected from the COF-505 (Fig. 3C) by combining specimen tilt and electron-beam tilt in the range of –41.3° to +69.1° with a beam-tilt step of 0.2°. From the acquired data set, 3D reciprocal lattice of COF-505 was constructed that was identified as a *C*-centered orthorhombic Bravais lattice. The unit-cell parameters were a = 18.9 Å, b = 21.3 Å, c = 30.8 Å, and V = 12399 $Å^3$, which were used to index reflections observed in both powder x-ray diffraction (PXRD) pattern and Fourier diffractograms of high-resolution transmission electron microscopy (HRTEM) images (Fig. 3D to F). The unit-cell parameters were further refined to be a = 18.6 Å, b = 21.4 Å, c = 30.2 Å, and V = 12021 $Å^3$ by Pawley refinement of PXRD pattern (Fig. 3G). The observed reflection conditions were summarized as *hkl*: $h+k = 2n$; *hk*0: $h,k = 2n$; *h*0*l*: $h = 2n$; and 0*kl*: $k = 2n$, which suggests five possible space groups—*Cm*2*a* (no. 39), *Cmma* (no. 67), *Cmca* (no. 64), *Cc*2*a* (no. 41), and *Ccca* (no. 68). Three of them—*Cm*2*a*, *Cmma*, and *Ccca*—were excluded because their projected plane group symmetries along [1-10] did not coincide with that of the HRTEM image, *pgg* (Fig. 3E). Furthermore, by performing Fourier analysis of the HRTEM images and imposing symmetry to the reflections, Cu(I) positions were

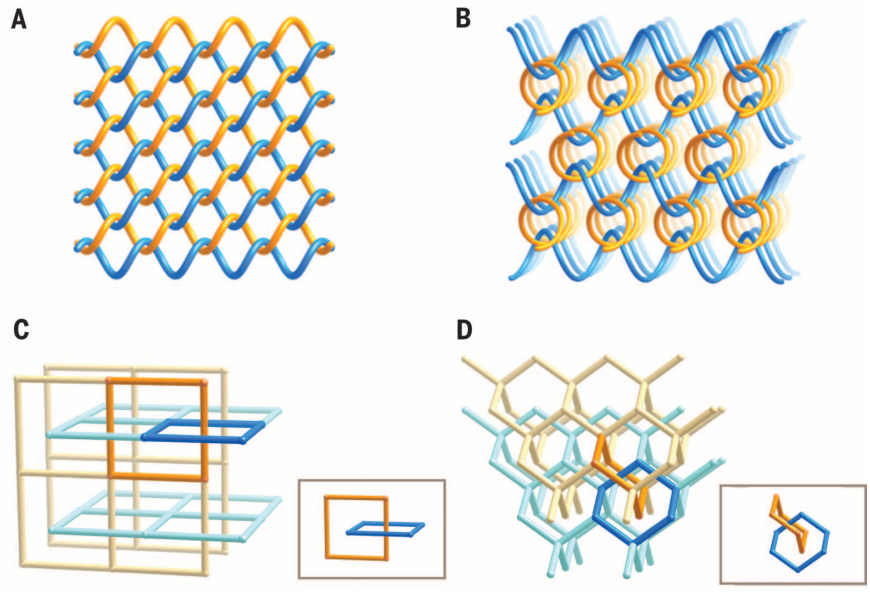

Fig. 1. Weaving and entanglement. Illustrations of weaving of threads in two (**A**) and three (**B**) dimensions, compared with entanglements of sheets (**C**), 3D arrangements (**D**), and their interlocking of rings (insets).

determined from the reconstructed 3D potential map (Fig. 3F). The structure of COF-505 was built in Materials Studio by putting $Cu(PDB)_2$ units at copper positions and connecting them through biphenyl (reacted BZ) molecules. The chemical compositions were determined by elemental analysis; therefore, once the number of copper atoms in one unit cell was obtained, the numbers of other elements in one unit cell were also determined, which indicates that the unit-cell framework is constructed by 8 $Cu(PDB)_2$ and 16 biphenyl units. However, symmetry operations of the space group *Cmca* require two PDB units connected to one copper onto a mirror plane perpendicular to *a* axis, which is not energetically favorable geometry. The final space group determined, *Cc2a*, was used to build and optimize a structure model. The PXRD pattern calculated from this model is consistent with the experimental pattern of activated COF-505 (*12*).

According to the refined model, COF-505 crystallizes in a diamond (**dia**) network with the distorted tetrahedral building units $Cu(PBD)_2$ and biphenyl linkers BZ linked through trans imine bonds. As a result, covalently linked adamantane-like cages 19 by 21 by 64 Å are obtained and elongated along the *c* axis (dimensions are calculated based on Cu-to-Cu distances). This size allows two diamond networks of identical frameworks to form the crystal. These frameworks are mutually interpenetrating (when the Cu centers are considered) in COF-505 crystals along the *c* direction, where the frameworks are related by a C_2 rotation along the *b* axis, leaving sufficient space for BF_4^- counterions (*20*). We note that when the structure is demetalated, as demonstrated below, the COF is mutually woven (Fig. 2B).

Fundamentally, each of the threads making up the framework is a helix (Fig. 4A). For clarity, only a fragment of one weaving framework is shown. The helices are entirely made of covalently linked organic threads. As expected, they are weaving and being held by Cu(I) ions at their points of registry (Fig. 4B). These threads are propagating in two different directions along [110] and [–110]. Although the helices are chemically identical, they have opposite chirality, giving rise to an overall racemic weaving framework (Fig. 4, C and D) of the same topology as in Fig. 1B. We note that in the context of reticular chemistry, the points of registry play an important role in crystallizing otherwise difficult-to-crystallize threads and to do so into 2D or 3D frameworks. This arrangement is in stark contrast to the parallel manner in which such 1D objects commonly pack in the solid state.

The COF-505 structure is a woven fabric of helices, so we sought to remove the Cu centers and examine the properties of the material before and after demetalation. Heating COF-505 in a KCN methanol-water solution (*8*) yielded a demetalated material. Using inductively coupled plasma (ICP) analysis, we found that 92 to 97% of the Cu(I) copper ions had been removed (*12*). The dark brown color of COF-505 [from the copper-phenanthroline metal-to-ligand charge transfer (MLCT) (*21*)] changed to pale yellow as

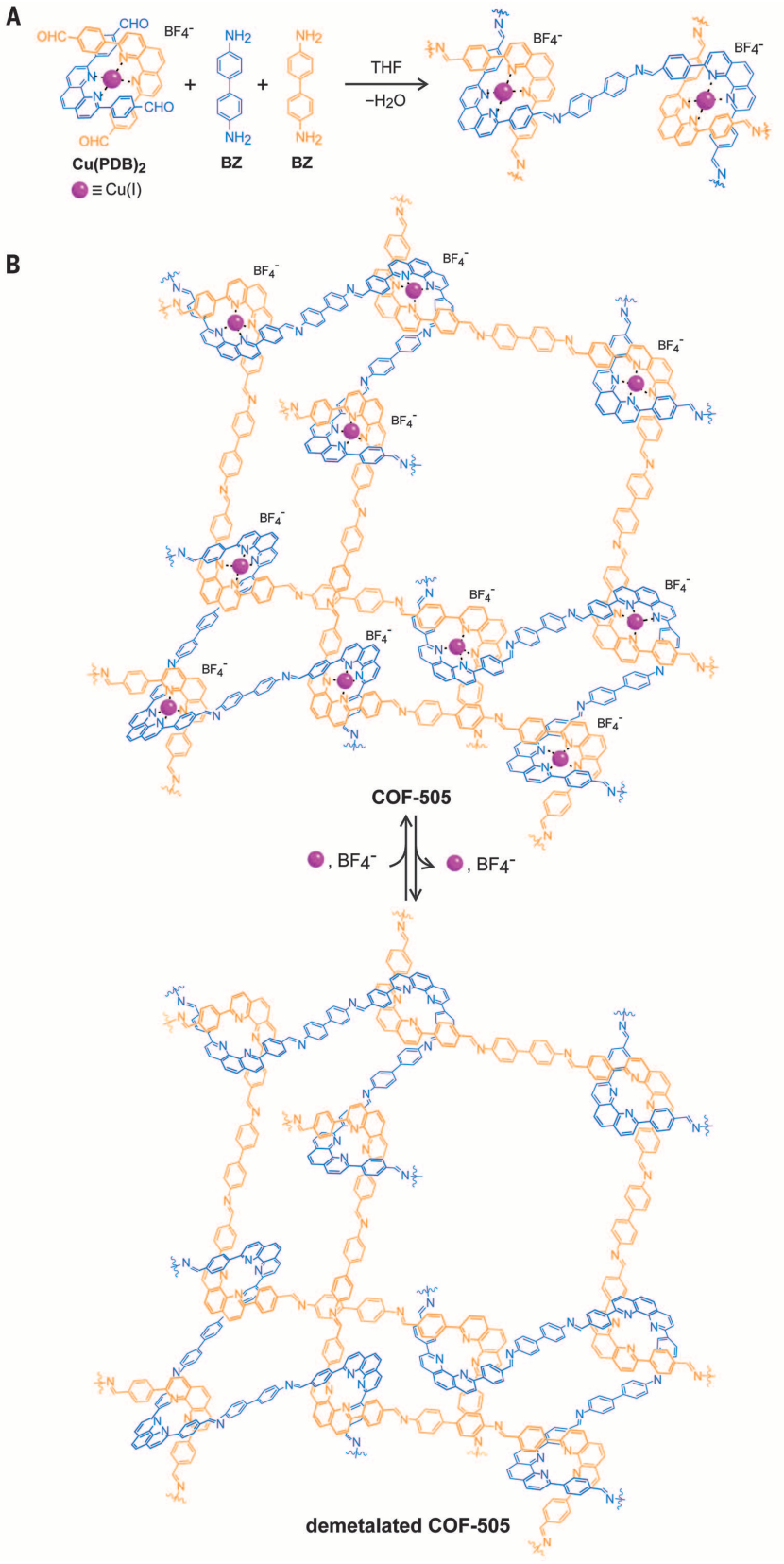

Fig. 2. A general strategy for the design and synthesis of weaving structures. COF-505 was constructed from organic threads using copper(I) as a template (**A**) to make an extended weaving structure (**B**), which can be subsequently demetalated and remetalated.

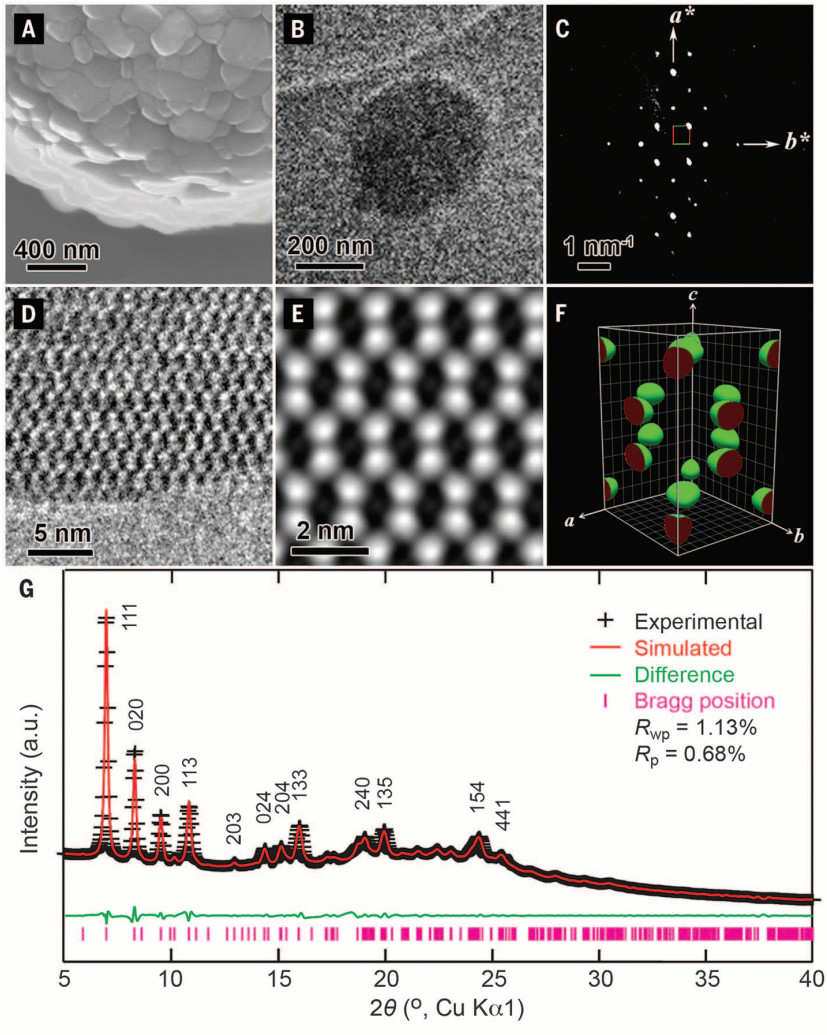

Fig. 3. Morphology and electron microscopy studies of COF-505. (**A**) Crystallites aggregated on a crystalline sphere observed by SEM. (**B**) TEM image of a single sub-μm crystal used for 3D-EDT. (**C**) 2D projection of the reconstructed reciprocal lattice of COF-505 obtained at 298 K from a set of 3D-EDT data. (**D**) HRTEM image of COF-505 taken with the [1-10] incidence. (**E**) 2D projected potential map obtained by imposing *pgg* plane group symmetry on Fig. 1D. (**F**) Reconstructed 3D electrostatic potential map (threshold, 0.8). (**G**) Indexed PXRD pattern of the activated sample of COF-505 (black) and the Pawley fitting (red) from the modeled structure.

demetalation proceeded (*12*). Although the crystallinity of demetalated material decreased compared with COF-505, SEM images show similar morphology before and after demetalation (*12*). Additionally, the imine linkages were also maintained; the FT-IR peaks at 1621 and 1195 cm^{-1} (*12*) are consistent with those of COF-505 (1621 and 1196 cm^{-1}, respectively). Furthermore, the material could be remetalated with Cu(I) ions by stirring in a $CH_3CN/CHCl_3$ solution of $Cu(CH_3CN)_4(BF_4)$ to give back crystalline COF-505. This remetalated COF-505 has identical crystallinity to the original as-synthesized COF-505, as evidenced by the full retention of the intensity and positions of the peaks in the PXRD (*12*). In the FT-IR spectrum, the peak representing imine C=N stretch was retained (*12*), indicating that the framework is chemically stable and robust under such reaction conditions.

Given the facility with which demetalation can be carried out and the full retention of the structure upon remetalation can be achieved, we examined the elastic behavior of the metalated and demetalated COF-505. A single particle of each of these two samples was indented by a conical tip of an atomic force microscope (AFM), and the load-displacement curves were recorded for both loading and unloading process (*22*). The effective Young's moduli (neglecting the anisotropy of the elasticity) of the two COF-505 materials was ~12.5 and 1.3 GPa for the metalated and demetalated particles, respectively (*12*). Notably, this tenfold ratio in elasticity upon demetalation of COF-505 is similar to the elasticity ratio for porous MOFs to polyethylene (*23*). The distinct increase of elasticity could be attributed to the loose interaction between the threads upon removal of copper. Moreover, the elasticity of the original COF-505 could be fully recovered after the process of demetalation and remetalation, being facilitated by the structure of weaving helical threads that easily "zip" and "unzip" at their points of registry. The large difference in elasticity modulus is caused by loss of Cu(I) ions, which in total only represent a minute mole percentage (0.67 mol%) of the COF-505 structure.

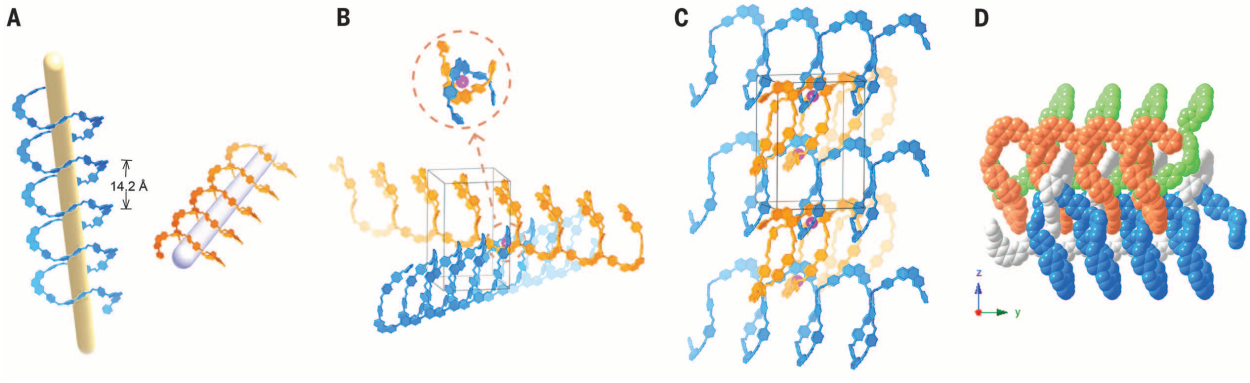

Fig. 4. Single-crystal structure of COF-505. The weaving structure of COF-505 consists of chemically identical helices (marked in blue and orange because they are of opposite chirality) with the pitch of 14.2 Å (**A**). The orange helices propagate in the [1-10] direction, whereas the blue helices propagate in the [110] direction with copper (I) ions as the points of registry (**B**). Neighboring blue helices are woven with the orange helices to form the overall framework (**C**). Blue and orange helices and their C_2 symmetry-related green and gray copies are mutually woven (**D**). Additional parallel helices in (C) and (D) are omitted for clarity.

REFERENCES AND NOTES

1. O. M. Yaghi *et al.*, *Nature* **423**, 705–714 (2003).
2. L. Carlucci, G. Ciani, D. M. Proserpio, *Coord. Chem. Rev.* **246**, 247–289 (2003).
3. B. Chen, M. Eddaoudi, S. T. Hyde, M. O'Keeffe, O. M. Yaghi, *Science* **291**, 1021–1023 (2001).
4. V. A. Blatov, L. Carlucci, G. Ciani, D. M. Proserpio, *Cryst. Eng. Comm.* **6**, 378–395 (2004).
5. S. R. Batten, R. Robson, *Angew. Chem. Int. Ed.* **37**, 1460–1494 (1998).
6. T. K. Maji, R. Matsuda, S. Kitagawa, *Nat. Mater.* **6**, 142–148 (2007).
7. C. O. Dietrich-Buchecker, J.-P. Sauvage, *Angew. Chem. Int. Ed. Engl.* **28**, 189–192 (1989).
8. C. O. Dietrich-Buchecker, J.-P. Sauvage, J. M. Kern, *J. Am. Chem. Soc.* **106**, 3043–3045 (1984).
9. M.-C. Jiménez, C. Dietrich-Buchecker, J.-P. Sauvage, *Angew. Chem. Int. Ed.* **39**, 3284–3287 (2000).
10. S. V. Pakhomova, M. A. Proskurnin, V. V. Chernysh, M. Y. Kononets, E. K. Ivanova, *J. Anal. Chem.* **56**, 910–917 (2001).
11. M. Linke *et al.*, *J. Am. Chem. Soc.* **122**, 11834–11844 (2000).
12. Materials and methods are available as supplementary materials on *Science* Online.
13. M. T. Miller, P. K. Gantzel, T. B. Karpishin, *Inorg. Chem.* **37**, 2285–2290 (1998).
14. Y.-B. Zhang *et al.*, *J. Am. Chem. Soc.* **135**, 16336–16339 (2013).
15. F. J. Uribe-Romo *et al.*, *J. Am. Chem. Soc.* **131**, 4570–4571 (2009).
16. X. Wu, K. W. Zilm, *J. Magn. Reson.* **102**, 205–213 (1993).
17. M. Gemmi, P. Oleynikov, *Z. Kristallogr.* **228**, 51–58 (2013).
18. E. Mugnaioli *et al.*, *Angew. Chem. Int. Ed.* **51**, 7041–7045 (2012).
19. Q. Sun *et al.*, *J. Mater. Chem. A* **2**, 17828–17839 (2014).
20. E. V. Alexandrov, V. A. Blatov, D. M. Proserpio, *Acta Crystallogr. A* **68**, 484–493 (2012).
21. D. V. Scaltrito, D. W. Thompson, J. A. O'Callaghan, G. J. Meyer, *Coord. Chem. Rev.* **208**, 243–266 (2000).
22. W. C. Oliver, G. M. Pharr, *J. Mater. Res.* **19**, 3–20 (2004).
23. J. C. Tan, A. K. Cheetham, *Chem. Soc. Rev.* **40**, 1059–1080 (2011).

ACKNOWLEDGMENTS

The structures of COF-505 and Cu(PDB)$_2$(BF$_4$) are available free of charge from the Cambridge Crystallographic Data Centre under the reference numbers CCDC-1434851 and CCDC-1434852, respectively. This research was supported by BASF SE (Ludwigshafen, Germany) for synthesis and basic characterization, and the U.S. Department of Defense, Defense Threat Reduction Agency (HDTRA 1-12-1-0053) for mechanical properties. We thank C. Canlas for his assistance with solid-state NMR and A. Schöedel (Yaghi group), B. Zhang, and Y. Liu (Molecular Foundry, Lawrence Berkeley National Laboratory) for helpful discussions. This work was also supported by the Spanish Ministry of Economy and Competitiveness through the Juan de la Cierva program (F.G.); a Grant-in-Aid for Scientific Research (C) (25390023) and JST Research Acceleration Program (Z.L. and K.S.); grants from Vetenskapsrådet (Y.M. and P.O.) and JEOL Ltd (P.O.), Japan; EXSELENT and 3DEM-Natur, Sweden (O.T.); and BK21Plus, Korea (O.T.). Beamline 7.3.3 of the Advanced Light Source is supported by the Director of the Office of Science, Office of Basic Energy Sciences, of the U.S. Department of Energy under contract DE-AC02-05CH11231. The AFM study was supported by the National Science Foundation (NSF) (grant DMR-1344290). The data reported in the paper are presented in the supplementary materials.

SUPPLEMENTARY MATERIALS

www.sciencemag.org/content/351/6271/365/suppl/DC1
Materials and Methods
Figs. S1 to S21
Tables S1 to S4
Reference (*24*)

8 September 2015; accepted 25 November 2015
10.1126/science.aad4011

PHOTOPHYSICS

Direct observation of triplet energy transfer from semiconductor nanocrystals

Cédric Mongin,[1] Sofia Garakyaraghi,[1] Natalia Razgoniaeva,[2] Mikhail Zamkov,[2] Felix N. Castellano[1]*

Triplet excitons are pervasive in both organic and inorganic semiconductors but generally remain confined to the material in which they originate. We demonstrated by transient absorption spectroscopy that cadmium selenide semiconductor nanoparticles, selectively excited by green light, engage in interfacial Dexter-like triplet-triplet energy transfer with surface-anchored polyaromatic carboxylic acid acceptors, extending the excited-state lifetime by six orders of magnitude. Net triplet energy transfer also occurs from surface acceptors to freely diffusing molecular solutes, further extending the lifetime while sensitizing singlet oxygen in an aerated solution. The successful translation of triplet excitons from semiconductor nanoparticles to the bulk solution implies that such materials are generally effective surrogates for molecular triplets. The nanoparticles could thereby potentially sensitize a range of chemical transformations that are relevant for fields as diverse as optoelectronics, solar energy conversion, and photobiology.

Semiconductor nanocrystals represent an important class of stable light-emitting materials that can be systematically tuned as a result of size-dependent quantum confinement, producing intense absorptions and photoluminescence ranging from the ultraviolet (UV) to the near-infrared (near-IR) (*1*, *2*). Their prominence continues to expand, owing to extensive optoelectronic, photochemical, and biomedical applications (*3*–*9*). Substantial research effort has been expended on funneling energy into these nanomaterials to produce enhanced photoluminescence via Förster transfer and on exploiting the energized semiconductor nanocrystals to deliver or accept electrons from substrates (*10*–*14*), sometimes en route to solar fuels photosynthesis (*15*–*18*). Tabachnyk *et al.* and Thompson *et al.* independently demonstrated the reverse triplet energy transfer process to that described here, wherein molecular organic semiconductors transfer their triplet energy to PbSe and PbS nanocrystals in thin films that interface both materials (*19*, *20*). However, the extraction of triplet excitons from semiconductor quantum dots and related inorganic nanomaterials remains largely unexplored. Semiconductor nanocrystals potentially offer considerable advantages over molecular photosensitizers in terms of facile preparative synthesis, photostability, size-tunable electronic and photophysical properties, high molar extinction coefficients, and trivial postsynthesis functionalization. Moreover, the inherently large (and energy-consuming) singlet-triplet energy gaps characteristic of molecular sensitizers can be circumvented by using nanomaterials with ill-defined spin quantum numbers and closely spaced (1 to 15 meV) excited-state energy levels (*21*–*24*). The broadband light-absorption properties of inorganic semiconductors are extendable into the near-IR region and can potentially be exploited for numerous triplet excited-state reactions, thus enabling stereoselective photochemical synthesis, photoredox catalysis, singlet oxygen generation, photochemical upconversion, and excited-state electron transfer. Here we provide definitive experimental evidence that triplet energy transfer proceeds rapidly and efficiently from energized semiconductor nanocrystals to surface-anchored molecular acceptors. Specifically, CdSe nanocrystals are shown to serve as effective surrogates for molecular triplet sensitizers and can readily transfer their triplet excitons to organic acceptors at the interface with near-quantitative efficiency.

The nanoparticle-to-solution triplet exciton transfer strategy that we implemented is shown schematically in Fig. 1; this diagram depicts all of the relevant photophysical processes and the associated energy levels promoting material-to-molecule triplet exciton migration. We employed oleic acid (OA)–capped CdSe nanocrystals (CdSe-OA) as the light-absorbing triplet sensitizer in conjunction with 9-anthracenecarboxylic acid (ACA) and 1-pyrenecarboxylic acid (PCA) as triplet acceptors in toluene. The carboxylic acid functionality enables adsorption of these chromophores on the CdSe surface through displacement of the OA capping ligands; subsequent washing steps isolate the desired CdSe/ACA or CdSe/PCA donor/acceptor systems. Selective green light excitation of CdSe/ACA or CdSe/PCA sensitizes triplet exciton migration from the semiconductor to the surface-bound molecular acceptor. We directly visualized this interfacial Dexter-like

[1]Department of Chemistry, North Carolina State University, Raleigh, NC 27695-8204, USA. [2]Department of Physics and Center for Photochemical Sciences, Bowling Green State University, Bowling Green, OH 43403, USA.
***Corresponding author. E-mail: fncastel@ncsu.edu**